Surface morphology and composition studies in InGaN/GaN film grown by MOCVD*

Tao Tao(陶涛), Zhang Zhao(张曌), Liu Lian(刘炼), Su Hui(苏辉), Xie Zili(谢自力)†, Zhang Rong(张荣), Liu Bin(刘斌), Xiu Xiangqian(修向前), Li Yi(李毅), Han Ping(韩平), Shi Yi(施毅), and Zheng Youdou(郑有炓)

Key Laboratory of Advanced Photonic and Electronic Materials, School of Electronics Science and Engineering, Nanjing University, Nanjing 210093, China

Abstract: InGaN films were deposited on (0001) sapphire substrates with GaN buffer layers under different growth temperatures by metalorganic chemical vapor deposition. The In-composition of InGaN film was approximately controlled by changing the growth temperature. The connection between the growth temperature, In content, surface morphology and defect formation was obtained by X-ray diffraction, scanning electron microscopy (SEM) and atomic force microscopy (AFM). Meanwhile, by comparing the SEM and AFM surface morphology images, we proposed several models of three different defects and discussed the mechanism of formation. The prominent effect of higher growth temperature on the quality of the InGaN films and defect control were found by studying InGaN films at various growth temperatures.

Key words: InGaN film; MOCVD; surface morphology; V-defects
DOI: 10.1088/1674-4926/32/8/083002 **EEACC:** 2520

1. Introduction

Since GaN based light-emitting devices have been widely used and extensively studied in recent years, the manufacture technology of blue–green LEDs has been highly developed. Today, the third generation of GaN based semiconductor materials and devices are gradually being brought to industrialization[1−4]. And the progress in study of InGaN materials and InGaN/GaN quantum well structures is remarkable. The efficiency of InGaN/GaN LEDs is improved by the localization of charge carriers in InGaN films, which is based on fluctuations in In-composition and thickness or phase separation of InN. However, disputes about the mechanism of luminescence in group III nitrides semiconductors still exist[2, 5−16]. Those dislocations may affect the charge carriers dramatically, most of which are threading dislocations, defects of some kind and fluctuations in thickness. Meanwhile，due to the quantum-confined Stark effect induced by piezoelectric fields in strained InGaN/GaN films[17−20], the radiative recombination dynamics are still complicated. Whatever the relationship between the surface morphology of InGaN/GaN films and luminescence efficiency is discussed in each theory above.

Recently, there has been great interest in inverted hexagonal pyramid defects (V-defects) on the surface or interface of InGaN/GaN films[6, 7, 20]. The Sonderegger group[10] discussed the influence of luminescence on surface fluctuations caused by mountains and valleys. However, there are still some issues that can't be explained by the theory of charge carrier localization. Studies on the surface morphology of InGaN/GaN quantum wells are still inevitable. Herein, InGaN/GaN heterostructure films were prepared by metalorganic chemical vapor deposition (MOCVD) under various growth temperatures. Seven samples were investigated by means of AFM, XRD and SEM. The connections between growth temperature, film quality, surface morphology and In-composition were gathered and analyzed.

2. Experiment

Seven InGaN samples, labeled A, B, C, D, E, F, and G, were grown on sapphire (0001) with GaN buffer layers under different growth temperatures by a Thomas Swan metal-organic chemical vapor deposition (MOCVD) system. Prior to the growth, those substrates were calcined at 1180 ℃ for 600 s in a hydrogen atmosphere. Trimethylindium (TMIn), trimethylgallium (TMGa), and ammonia (NH_3) were used as precursors, with H_2 and N_2 as the carrier gas to allow for the growth of GaN and InGaN. The growth temperature T_G amounted to 570 ℃ and 1100 ℃ for the GaN nucleation and buffer layer. Due to the dilemma of thermal stability in InGaN films at high temperatures, the reactor temperature for InGaN film was in the 780–830 ℃ range in order to balance the desorption of indium and efficient ammonia cracking. The typical thickness of GaN buffer layers and InGaN films is about 2.6–2.7 μm and 200 nm, respectively. The other growth parameters, such as reactor pressure, carrier gases' flow rate, and flow rate ratio, remained the same in every sample preparation

* Project supported by the Special Funds for Major State Basic Research Project, China (No. 2011CB301900), the Hi-Tech Research Project (No. 2009AA03A198), the National Natural Science Foundation of China (Nos. 60990311, 60721063, 60906025, 60936004), the Natural Science Foundation of Jiangsu Province, China (Nos. BK2008019, BK2009255, BK2010178), and the Research Funds from NJU-Yangzhou Institute of Opto-Electronics, China.

† Corresponding author. Email: xzl@nju.edu.cn

Received 27 December 2010, revised manuscript received 6 April 2011

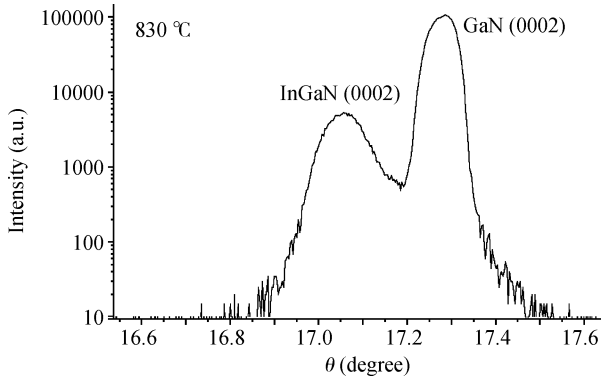

Fig. 1. X ray diffraction spectrum of InGaN sample grown at 830 ℃. Diffraction peaks of GaN (0002) and InGaN (0002) are clearly visible.

Table 1. In-composition parameters of InGaN samples.

Sample	Growth temperature (℃)	In composition
A	780	0.233
B	790	0.216
C	800	0.201
D	810	0.182
E	820	0.156
F	825	0.15
G	830	0.132

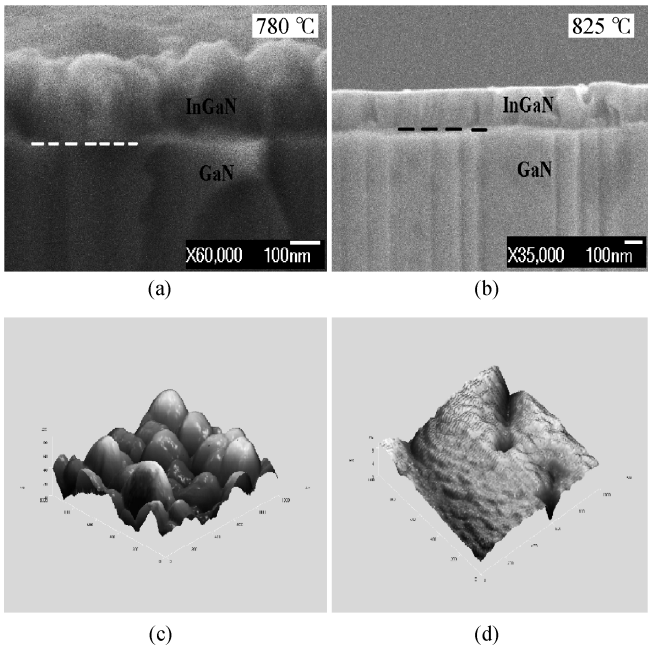

Fig. 2. Cross-sectional SEM scans of InGaN samples grown at (a) 780 ℃ and (b) 825 ℃. AFM surface morphology images of InGaN samples grown at (c) 810 ℃ and (d) 830 ℃.

in order to illustrate the effect of growth temperature only. Information about In-composition was approximately obtained from XRD data. Meanwhile, according to the comparison between scans of SEM and AFM surface morphology, the influence of the growth temperature was discussed.

3. Results and discussion

All InGaN alloy samples were measured by PANalytical X'Pert Pro MRD triple-axis X-ray diffraction. Figure 1 plots a ω–2θ scan of X-ray results of an InGaN film grown at 830 ℃. The diffraction peaks of GaN (0002) and InGaN (0002) are clearly visible. The diffraction peak positions of each sample are slightly different. According to Vegard's law, the In content x can be approximately calculated, which is shown in Table 1 assuming that those InGaN films are fully relaxed since they were grown at a high temperature, such as 800 ℃ around and the thickness of those films are greater than the critical layer thickness in the InGaN/GaN heterostructures[16, 21–24].

$$d(\mathrm{InGaN}_{(0002)}) = xd(\mathrm{InN}_{(0002)}) + (1-x)d(\mathrm{GaN}_{(0002)}). \quad (1)$$

From sample A to sample G, the In-composition drops as the growth temperature increases. The results are similar to lots of publications[1, 5, 12–16, 25]. It is widely accepted that the manufacture of In-rich InGaN film is quite hard to achieve due to the high saturation vapour pressure of InN. The higher the temperature goes, the more often the desorption of indium occurs. On the other hand, the thickness of InGaN films will also decrease slightly with increasing temperature.

The surface morphology of an InGaN/GaN single quantum well will be affected by lots of parameters, such as the reactor temperature, the carrier gas flow rate, the flow rate ratio and the substrate material. Therefore, the mechanism of surface formation is still complex. In this study, we aimed at the growth temperature rather than others. Surface images with different characteristics were obtained by AFM and SEM. Cross-sectional SEM scans of sample A and E are shown in Figs. 2(a) and 2(b), respectively. The surface of sample A is quite rough in Fig. 2(a). There are lots of mounts and valleys, therefore the thickness of the InGaN films changes frequently. The surface of sample E looks different: it looks like an arrangement of plains. Because of the typical step-flow mode of GaN growth, the interface between InGaN and GaN is smooth. Furthermore, the AFM surface morphology images can be used as a reference to identify the difference between the surfaces of samples grown at high temperature and low temperature. From the AFM pictures, shown in Figs. 2(c) and 2(d), it is easy to pinpoint the rough face of sample D within a 1×1 μm^2 area. Fluctuations in thickness can reach around 40 nm in sample D, while it is about a dozen in sample G at most. By comparison, growth in 2 dimensional step-flow mode at low temperature and in 3 dimensional island mode at high temperature are observed in Figs. 2(c) and 2(d). Various groups have proposed several reasons[12, 13, 15, 25, 26]. First, the diffusion distance of atoms in the growth process increases when the temperature of the substrates rises. A longer diffusion distance of the atoms represents a greater ability of movement on the surface of the InGaN film during the process. Atoms can replace some defects and dislocations by means of moving ahead of the film formation. And then phase-separation of In can decrease. Second, the efficiency of ammonia cracking may be improved by raising the growth temperature. The concentration of N^+ is enhanced, so it becomes much easier to combine In, Ga and N into In–N bonds or Ga–N bonds. The utilization of gas resources becomes efficient. Finally, InN material decomposes easily due to the high saturation vapour pressure. The In-rich

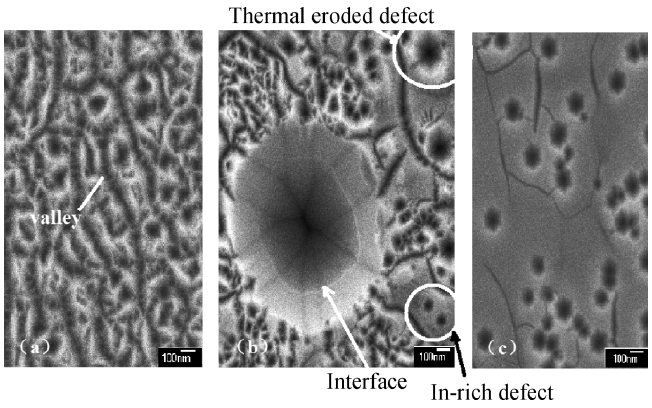

Fig. 3. SEM surface morphology images of InGaN samples grown at (a) 780 ℃, (b) 810 ℃ and (c) 830 ℃.

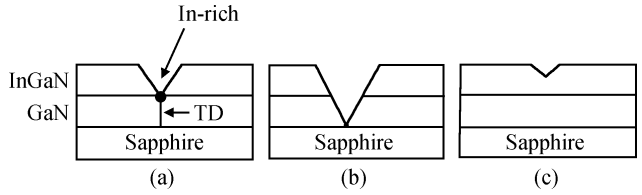

Fig. 4. Three models of InGaN defects. (a) In-rich defect. (b) Big V-defect. (c) Thermal-eroded defect.

areas on the surface of the InGaN films will decompose into the reactor atmosphere easily, while the other areas remain the same. Therefore, the number of In-rich areas decreases. All of these reasons lead to a promoted surface of the InGaN film.

In Fig. 3, surface morphology images of samples A, D and G show different characters. The surfaces of samples grown at low temperature are full of mounts and valleys, while the high temperature samples are different. These experimental data also prove the above discussion about cross-sectional SEM images. However, we believe that the dynamics of valley formation in sample A and sample G are distinct. At low temperatures, InGaN films grew as a 3 dimensional island model. Islands of InGaN material nucleated at first and grew bigger into mounts later. As the mounts grew bigger and bigger, they linked together. Therefore, the number of valleys formed and the surface morphology of sample A became complicated, as shown in Fig. 3(a). On the other hand, at high temperature, InGaN films formed as a 2 dimensional step-flow model. This is also proved by the AFM pictures above. Valleys on the surface of sample G come from the strain, which is caused by crystal mismatch and a different thermal expansion coefficient between the InGaN and GaN materials. After the strain was released by valleys and defects, a plane formed in good condition. This is also supported by some reports[6, 10].

Three kinds of defect can be found out in Fig. 3. First of all, the big V shaped pits (also called V-defects) can be easily seen in Fig. 3(b). The size of this kind of pit can reach several hundred nanometers. The interface between the InGaN film and the GaN buffer layer is pointed out by the white arrow. After calculating the angle and depth of the big V-defects, we believe that those pits originated at the GaN buffer layer or the interface between the sapphire and GaN buffer layer, as shown in Fig. 4(b). Because no source of In was applied in the reaction process of GaN buffer layer growth, those defects originated from the GaN buffer layer itself rather than In-rich dots. From the experimental data, 6 identical sidewalls on $(10\bar{1}1)$ planes and an inverted hexagonal pyramid can be clearly observed as characters of big V-defects. Another kind of defect is marked by a white circle at the top right corner of Fig. 3(b). We call this kind of defects a thermal eroded pit. Because the formation of InGaN films is a combination of growth and dissolution in the process, these pits originated in the process of InGaN film growth. Therefore, present of thermal eroded pits are quite common. Otherwise, the size of these pits won't exceed 150 nm, as shown in Figs. 3(b) and 3(c). By comparing the images of samples A and G, it is found that the number of thermal eroded pits increase with rising growth temperature. Figure 4(c) illustrates the model of thermal eroded pits. These look like small V-defects and had no concern with In-concentration or threading dislocations. Figure 4(a) plots the model of the last kind of defects. And those defects are marked by a white circle at the right bottom corner of Fig. 3(b). We propose that these defects are In-rich dots. The mechanism of In-rich dot formation remains much more complex than others. Some groups have investigated the V-defects by means of TEM and STEM. They proved that the origin of V-defects is threading dislocation (TD)[6–8, 10, 13, 20, 27]. Stacking faults, edge TDs and mixed TDs are also believed to be potential origins[14]. It is widely accepted that the facets of V-defects are the $(10\bar{1}1)$ plane and the V-defects are usually associated with In-rich dots[2, 5–7, 9, 10, 13, 14, 20, 27–29]. We believe that threading dislocations work as a habitat for indium. After In is deposited at the dislocations, InGaN material grew with the sidewall on the $(10\bar{1}1)$ plane in the vicinity of the In-rich dots. Thus V shaped defects formed, as shown in Fig. 4(a). It is known that TDs are nonradioactive recombination centers, and fluctuations in thickness will influence the radiative features. So all of these 3 kinds of defects should act differently in radiative behavior.

4. Conclusions

In summary, In-composition of InGaN films was approximately managed within the arrangement of 0.23–0.13 by means of changing the growth temperature. The influences of growth temperature on the In content and surface morphology were analyzed using XRD, SEM and AFM measurements. Their different characteristic surface morphology was compared. We proposed a 2 dimensional step-flow model and a 3 dimensional island model to illustrate the formation of mounts and valleys. Three kinds of defects (big V-defects originated at the GaN buffer layers/V-shaped thermal eroded defects and In-rich dots) were proposed and discussed. The characteristics of each kind of defect were analyzed. Comparison among the SEM and AFM images illustrate the improvement of InGaN film quality and surface morphology by the method of choosing the right growth temperature.

References

[1] Zhu Lihong, Liu Baolin, Zhang Baoping. Study of optical characteristics of InGaN/GaN MQW LED depended on growth tem-

perature. Semiconductor Optoelectronics, 2008, 29(2): 165
[2] Hangleiter A, Hitzel F, Netzel C, et al. Suppression of nonradiative recombination by V-shaped pits in GaInN/GaN quantum wells produces a large increase in the light emission efficiency. Phys Rev Lett, 2005, 95: 127402
[3] Rice J H, Robinson J W, Jarjour A, et al. Temporal variation in photoluminescence from single InGaN quantum dot. Appl Phys Lett, 2004, 84(20): 4110
[4] Kumar M S, Park J Y, Lee Y S, et al. Improved internal quantum efficiency of green emitting InGaN/GaN multiple quantum wells by in preflow for InGaN well growth. Jpn J Appl Phys, 2008, 47(2): 839
[5] Zhu L, Liu B. Optical properties studies in InGaN/GaN multiple-quantum well. Solid-State Electron, 2009, 53: 336
[6] Yoshikawa M, Murakami M, Ishida H, et al. Characterizing nanometer-sized V-defects in InGaN single quantum well films by high-spatial-resolution cathodoluminescence spectroscopy. Appl Phys Lett, 2009, 94(13): 1908
[7] Cherns D, Henley S J, Ponce F A. Edge and screw dislocations as nonradiative centers in InGaN/GaN quantum well luminescence. Appl Phys Lett, 2001, 78(18): 2691
[8] Ting S M, Ramer J C, Florescu D I, et al. Morphological evolution of InGaN/GaN quantum-well heterostructures grown by metalorganic chemical vapor deposition. J Appl Phys, 2003, 94(3): 1461
[9] Arif R A, Zhao H, Ee Y K, et al. Spontaneous emission and characteristics of staggered InGaN quantum well light-emitting diodes. J Quantum Electron, 2008, 44(6): 573
[10] Sonderegger S, Feltin E, Merano M, et al. High spatial resolution picosecond cathodoluminescence of InGaN quantum wells. Appl Phys Lett, 2006, 89: 232109
[11] Park I K, Kwon M K, Baek S H, et al. Enhancement of phase separation in the InGaN layer for self-assembled In-rich quantum dots. Appl Phys Lett, 2005, 87: 061906
[12] Xu Feng, Wu Zhenlong, Shao Yong, et al. Study of InGaN films grown by MOCVD. Micronanoelectron Technol, 2009, 46(5): 274 (in Chinese)
[13] Kumar M S, Lee Y S, Park J Y, et al. Surface morphological studies of green InGaN/GaN multi-quantum wells grown by using MOCVD. Mater Chem Phys, 2009, 113(1): 192
[14] Jahn U, Brandt O, Luna E, et al. Carrier capture by threading dislocations in (In,Ga)N/GaN heteroepitaxial layers. Phys Rev B, 2010, 81(12): 125314
[15] Liu B, Luo W, Zhang R, et al. Growth of In-rich and Ga-rich InGaN alloys by MOCVD and fabrication of InGaN-based photoelectrodes. Phys Status Solidi C, 2010, 7(7/8): 1817
[16] Qin Z, Chen Z, Tong Y, et al. Estimation of InN phase inclusion in InGaN films grown by MOVPE. Appl Phys A, 2002, 74: 655
[17] Lefebvre P, Morel A, Gallart M, et al. High internal electric field in a graded-width InGaN/GaN quantum well: accurate determination by time-resolved photoluminescence spectroscopy. Appl Phys Lett, 2001, 78(9): 1252
[18] Takeuchi T, Sota S, Katsuragawa M, et al. Quantum-confined Stark effect due to piezoelectric fields in GaInN strained quantum wells. Jpn J Appl Phys, 1997, 36: L382
[19] Winkelnkemper M, Schliwa A, Bimberg D. Interrelation of structural and electronic properties in $In_xGa_{1-x}N$/GaN quantum dots using an eight-band $k\cdot p$ model. Phys Rev B, 2006, 74: 155322
[20] Watanabe K, Yang J R, Huang S Y, et al. Formation and structure of inverted hexagonal pyramid defects in multiple quantum wells InGaN/GaN. Appl Phys Lett, 2003, 82(5): 718
[21] Kim C, Robinson I K. Critical thickness of GaN thin films on sapphire(0001). Appl Phys Lett, 1996, 69(16): 2358
[22] Parker C A, Roberts J C, Bedair S M. Determination of the critical layer thickness in the InGaN/GaN heterostructures. Appl Phys Lett, 1999, 75(18): 2776
[23] Wang B, Woo C H, Sun Q P, et al. Critical thickness for dislocation generation in epitaxial piezoelectric thin films. Philosophical Magazine, 2003, 83(31–34): 3753
[24] Behbehani M K, Piner E L, Liu S X, et al. Phase separation and ordering coexisting in $In_xGa_{1-x}N$ grown by metal organic chemical vapor deposition. Appl Phys Lett, 1999, 75(15): 2202
[25] Li Liang, Zhan Rong, Xie Zili, et al. Characterization of $In_xGa_{1-x}N$ layers grown by MOCVD. Journal of Synthetic Crystals, 2005, 34(6): 1118 (in Chinese)
[26] Chernyakov A E, Sobolev M M, Ratnikov V V, et al. Nonradiative recombination dynamics in InGaN/GaN LED defect system. Superlattices and Microstructures, 2009, 45(4/5): 301
[27] Wu X H, Elsass C R, Abare A, et al. Structural origin of V-defects and correlation with localized excitonic centers in InGaN/GaN multiple quantum wells. Appl Phys Lett, 1998, 72(6): 692
[28] Netzel C, Bremers H, Hoffmann L, et al. Emission and recombination characteristics of $Ga_{1-x}In_xN$/GaN quantum well structures with nonradiative recombination suppression by V-shaped pits. Phys Rev B, 2007, 76: 155322
[29] Kumar M S, Park J Y, Lee Y S, et al. Effect of barrier growth temperature on morphological evolution of green InGaN/GaN multi-quantum well heterostructures. J Phys D: Appl Phys, 2007, 40(17): 5050